Received: 29 July 2021 | Revised: 2 December 2021 | Accepted: 20 December 2021

DOI: 10.1096/fj.202101222R

THE FASEB JOURNAL

RESEARCH ARTICLE

Targeting of PFKFB3 with miR-206 but not mir-26b inhibits ovarian cancer cell proliferation and migration involving FAK downregulation

Carlotta Boscaro[1] | **Chiara Baggio**[1] | **Marcello Carotti**[2] | **Dorianna Sandonà**[2] | **Lucia Trevisi**[1] | **Andrea Cignarella**[3] | **Chiara Bolego**[1]

[1]Department of Pharmaceutical and Pharmacological Sciences, University of Padova, Padova, Italy

[2]Department of Biomedical Sciences, University of Padova, Padova, Italy

[3]Department of Medicine, University of Padova, Padova, Italy

Correspondence
Chiara Bolego, Department of Pharmaceutical and Pharmacological Sciences, University of Padova, Largo Meneghetti 2, I-35131 Padova, Italy.
Email: chiara.bolego@unipd.it

Funding information
Università degli Studi di Padova (University of Padova), Grant/Award Number: PRID 2018; Muscular Dystrophy Association (MDA), Grant/Award Number: 577888

Abstract

Few studies explored the role of microRNAs (miRNAs) in the post-transcriptional regulation of glycolytic proteins and downstream effectors in ovarian cancer cells. We recently showed that the functional activation of the cytoskeletal regulator FAK in endothelial cells is fostered by the glycolytic enhancer 6-phosphofructo-2-kinase/fructose-2,6-biphosphatase 3 (PFKFB3). We tested the hypothesis that miR-206 and mir-26b, emerging onco-suppressors targeting PFKFB3 in estrogen-dependent tumors, would regulate proliferation and migration of serous epithelial ovarian cancer (EOC) cells *via* common glycolytic proteins, i.e., GLUT1 and PFKFB3, and downstream FAK. PFKFB3 was overexpressed in SKOV3, and its pharmacological inhibition with 3-(3-pyridinyl)-1-(4-pyridinyl)-2-propen-1-one (3PO) significantly reduced cell proliferation and motility. Both miR-206 and miR-26b directly targeted *PFKFB3* as evaluated by a luciferase reporter assay. However, endogenous levels of miR-26b were higher than those of miR-206, which was barely detectable in SKOV3 as well as OVCAR5 and CAOV3 cells. Accordingly, only the anti-miR-26b inhibitor concentration-dependently increased PFKFB3 levels. While miR-206 overexpression impaired proliferation and migration by downregulating PFKFB3 levels, the decreased PFKFB3 protein levels related to miR-26 overexpression had no functional consequences in all EOC cell lines. Finally, consistent with the migration outcome, exogenous miR-206 and miR-26b induced opposite effects on the levels of total FAK and of its phosphorylated form at Tyr576/577. 3PO did not prevent miR-26b-induced SKOV3 migration. Overall, these results support the inverse relation between endogenous miRNA levels and their tumor-suppressive effects and suggest that restoring miR-206 expression represents a potential dual anti-PFKFB3/FAK strategy to control ovarian cancer progression.

KEYWORDS

FAK, miR-206, miR-26b, ovarian cancer cells, PFKFB3

Abbreviations: 3PO, 3-(3-pyridinyl)-1-(4-pyridinyl)-2-propen-1-one; E2, 17β-estradiol; EOC, epithelial ovarian cancer; FAK, focal adhesion kinase; FCS, fetal calf serum; GLUT1, Glucose transporter 1; miRNA, microRNA; PFKFB3, 6-phosphofructo-2-kinase/fructose-2,6-biphosphatase 3; qPCR, quantitative PCR.

1 | INTRODUCTION

Increased uptake and metabolism of glucose via glycolysis, even in the presence of oxygen, is a central metabolic hallmark of tumors. The rate of glycolytic flux is controlled at different levels and by different mechanisms including substrate availability, allosteric effectors, and expression of transporters and enzymes.[1,2] Overexpression of glycolytic enzymes and the glucose transporter GLUT1[2,3] has been reported in tumor cells and tissues and is considered to be an essential component of the malignant phenotype and invasive tumors such as ovarian cancer.[4–6]

The bifunctional enzyme 6-phosphofructo-2-kinase/fructose-2,6-biphosphatase 3 (PFKFB3) generates fructose-2,6-bisphosphate, a positive allosteric effector of 6-phosphofructo-1-kinase, one of the rate-limiting checkpoints of the glycolytic flux. PFKFB3 has been found to be overexpressed in human cancer cells and tissues, including ovarian cancer and its expression, correlates with more aggressive and invasive phenotypes although the precise mechanisms are unclear.[7,8] Moreover, PFKFB3 activity in ovarian cancer cells correlates with enhanced chemoresistance.[9] siRNA-targeted depletion of *PFKFB3* significantly increases cell death in mitotically arrested ovarian cancer cells.[10] Similarly, treatment with the PFKFB3 inhibitor 3-(3-pyridinyl)-1-(4-pyridinyl)-2-propen-1-one (3PO) reduces the growth of chemosensitive and chemoresistant ovarian cancer cell lines.[4] Remarkably, we and others showed that pharmacological inhibition of PFKFB3 reduces total levels of the cytosolic protein tyrosine kinase 2 (focal adhesion kinase, FAK), its phosphorylation at tyrosine 576/577 (FAK Y576/577) and cell motility, suggesting that the functional activation of FAK is fostered by glycolysis in endothelial and cancer cells.[11–13] Thus, PFKFB3 inhibition could have relevant effects on tumor progression due to both direct effects on tumor cells and indirect effects on endothelial cells of the tumor microenvironment.[14] However, little is known about the functional regulation of ovarian cancer cell motility by PFKFB3 and FAK.

The control of protein abundance at both transcriptional and post-transcriptional levels allows metabolic and functional cellular adaptation to environmental changes. The mechanisms dictating the functional expression of PFKFB3 and GLUT1 have been investigated in several studies, mainly in cancer cells.[2,3,15] We recently reported that 17β-estradiol (E2) rapidly increases PFKFB3 protein levels in a concentration-dependent manner without affecting PFKFB3 mRNA levels, suggesting that non-genomic mechanisms drive estrogen-boosted glycolysis in the vascular endothelium.[16] In addition, we reported that E2 increases PFKFB3 and GLUT1 protein abundance and angiogenesis acting at a post-transcriptional level, at least in part by inhibiting protein degradation.[17]

MicroRNAs (miRNAs) are small single-stranded non-coding RNA molecules that, once bound to complementary mRNA, cause inhibition of protein translation or mRNA degradation,[18] thereby acting as post-transcriptional regulators of protein abundance and functions. Emerging evidence recognizes miRNAs as novel players in glycolytic metabolism, mainly in pathological conditions.[19] Remarkably, in several cancer cell types, the amount of PFKFB3 and GLUT1 is regulated by the action of specific miRNAs, and deregulation of miRNA expression has been involved in estrogen-related cancers such as breast cancer. For example, E2 reduces endogenous miR-26b and miR-206 expression in the MCF-7 breast cancer cell line, which has been correlated with increased cell proliferation or migration.[20,21] Conversely, overexpression of these and other miRNAs downregulates PFKFB3 and/or GLUT1 protein levels, further supporting the relationship between levels of specific miRNAs, glycolysis, and tumor invasiveness.[21–23] Accordingly, miR-206 is significantly downregulated in estrogen receptor (ER) α^+ cells.[24,25] Several miRNAs are up or downregulated in ovarian cancer, suggesting that they play a role as a novel class of oncogenes or tumor-suppressor genes depending on the targets they regulate.[26] To the best of our knowledge, however, the role of miRNAs in the regulation of glycolytic proteins in this setting has not been investigated in detail.

Based on this background, we hypothesized that miR-206 and miR-26b would contribute to ovarian cancer cell malignant properties by post-transcriptional regulation of the common key glycolytic proteins GLUT1 and PFKFB3. Therefore, the objective of the present study was to assess the functional consequences of targeting glycolytic proteins, namely PFKFB3, in highly invasive serous epithelial ovarian cancer (EOC) cell lines, including estrogen-dependent SKOV3, OVCAR5, and estrogen-independent CAOV3. Specifically, we investigated the effects of miR-26b and miR-206 mimics and/or anti-miRs on cell proliferation and migration as well as the involvement of the signaling protein FAK.

2 | MATERIALS AND METHODS

2.1 | Cell culture

The human ovarian cancer cell lines SKOV3 and CAOV3 were purchased from the American Type Culture Collection (USA). OVCAR5 was purchased by Merck Life Science (Milan, Italy). All cell lines were maintained in RPMI 1640 (Sigma) supplemented with 10% fetal calf serum (FCS, Invitrogen, San Giuliano Milanese, Italy), 100 U/ml penicillin, and 100 μg/ml streptomycin (complete culture medium) at 37°C in a humidified 5% CO_2 atmosphere. Cells were used from passages 9 to 25. Human umbilical vein

endothelial cells (HUVECs) were isolated from normal-term umbilical cords as previously published.[27] The procedure was approved by Padua University Hospital Ethics Committee. Cells were grown at 37°C in a humidified 5% CO_2 atmosphere in a complete M199 medium (Sigma–Aldrich, Saint Louis, MO) supplemented with 15% FCS, gentamicin (40 μg/ml, Invitrogen), endothelial cell growth supplement (ECGS, 100 μg/ml), and heparin (100 UI/ml, Invitrogen). HUVECs were used from passages 2 to 6.

2.2 | MTT assay

SKOV3 (2.5×10^3 cells/well) were seeded in 96-well plates and treated as indicated in the Results section for 24–72 h in a complete culture medium. Selected experiments were performed using cells transfected with miR-26b or miR-206 mimics (37 nM) as detailed in the miRNA transfection method. Four hours before the incubation end, a 10 μl stock solution of 3-[4,5 dimethylthiazol-2-yl]-2,5 diphenyltetrazolium bromide (MTT, 5 mg/ml in PBS) was added to each well. Then, the medium was removed and formazan crystals were dissolved in 100 μl dimethylsulfoxide (DMSO). MTT reduction was quantified by measuring light absorbance with a multilabel plate reader (VICTOR2–Wallac) at 570–630 nm. Background absorbance values were subtracted from control wells (cell-free media). Cell viability is expressed as the raw optical density (OD) value and represents the mean value of three independent assays, performed in quadruplicate.

2.3 | Chemotaxis assay

Chemotaxis experiments were performed in a 48-well modified microchemotaxis chamber (Neuro Probe, Gaithersburg, MD, USA) using 8-μm nucleopore polyvinylpyrrolidone-free polycarbonate filters coated with 10 μg/ml collagen. Lower chambers were filled with RPMI supplemented with 0.1% bovine serum albumin (BSA, corresponding to basal migration) or 10% FCS as chemotactic stimuli, whereas the upper chambers were filled with 50 μl EOC cell line suspension (1.6×10^5 cells/ml in RPMI supplemented with 0.1% BSA). The PFFKB3 inhibitor 3PO (40 μM) was added in both the upper and lower compartment. Selected experiments were performed using cells transfected with miR-26b or miR-206 mimics (37 nM) in the presence or absence of 3PO as detailed in the miRNA transfection method. After 6 h incubation at 37°C, non-migrating cells on the upper filter surface were removed by scraping. Cells migrated to the lower filter side were stained with Diff-Quick stain (VWR Scientific Products, Bridgeport, NJ, USA), and densitometric analysis was performed using the Image J version 1.47 software (National Institutes of Health, NIH, USA). Each experiment was performed in sextuplicate. Results are reported as arbitrary units of OD and represent the mean values of three/four independent experiments.

2.4 | miRNA transfection

EOC cell lines (1×10^5/ml) were seeded in a complete culture medium. The next day (70% confluent), cells were transfected with miRNA mimics (miR-206 and miR-26b, 0.3–37 nM) or miRNA inhibitors (anti-miR-206 and anti-miR-26b, 0.3–37 nM) using Lipofectamine3000 (Life Technologies Inc.) for 72 h in RPMI 1640 with 5% FCS. At the end of the transfection period, western Blot, migration analysis, or MTT assay were performed. The miRNA mimic (miR-NC) or a miRNA inhibitor (anti-miR-NC, both 37 nM) with no homology to human gene sequences served as negative controls.

The following miRNA mimics or inhibitors (purchased from Sigma–Aldrich) were used:

MISSION® microRNA Mimic miR-26b-5p: cat. N° HMI0419.

MISSION® microRNA Mimic miR-206: cat. N° HMI0364.

MISSION® microRNA Negative Control 2, cat. N° HMC0003.

MISSION® Synthetic microRNA Inhibitor miR-26b-5p: cat. N° HSTUD0419.

MISSION® Synthetic microRNA Inhibitor miR-206: cat N° HSTUD0364.

MISSION® Synthetic microRNA Inhibitor, Negative Control 2, sequence from *C. elegans* with no homology to human gene sequences: cat N° NCSTUD002.

2.5 | Western blot

EOC cell lines (1×10^5/well) were seeded in 12-well plate dishes and transfected with miR-26b or miR-206 mimics (0.3–37 nM) as detailed in the miRNA transfection section. At the end of transfection, cells were lysed with 80 μl lysis buffer (phosphate-buffered saline supplemented with 1.2% Triton X-100, 1× Roche cOmplete Protease Inhibitor Cocktail (Roche Diagnostics, Mannheim, Germany), 2.5 mM NaF, 2 mM $Na_4P_2O_7$ (Sigma-Aldrich), 4 mM Na orthovanadate and 1 mM phenylmethanesulfonylfluoride). After centrifugation at 10 000 *g* for 15 min, the supernatants were collected. Protein quantification was performed using the bicinchoninic protein assay kit (Euroclone, Milan, Italy). Proteins (20–50 μg) were separated on SDS-PAGE and transferred onto Amersham Hybond-P polyvinylidene difluoride

membranes. Membranes were then blocked and probed using the following rabbit primary monoclonal antibodies at indicated dilutions: anti-PFKFB3, 1:5000; anti-GLUT1, 1:20 000; anti-glyceraldehyde-3-phosphate dehydrogenase, 1:10 000 (GAPDH; all from Abcam, Cambridge, UK); anti-phospho-FAK$^{Y576/577}$, 1:1000; anti-FAK, 1:1000 (Cell Signaling Technology, Danvers, MA, USA). After washing, the membranes were incubated with rabbit secondary horseradish peroxidase-conjugated antibodies (Vector Laboratories, Burlingame, CA). Bands were detected by chemiluminescence using the Westernbright™ Quantum (Advansta, Menlo Park, CA, USA). Images were acquired with Azure C400 (Azure biosystem, Dublin, CA, USA). Densitometric analysis of bands was performed using Image J version 1.47 software. Results are expressed as the percentage of controls and represent the mean values of three/five independent experiments.

2.6 | miRNA extraction and real-time qPCR

EOC cell lines (2×10^5 cells/well) were seeded in 35-mm dishes in a complete culture medium. After 48 h, the medium was replaced with fresh medium plus 5% FCS for 24 h. Cells were washed and the total miRNAs were extracted using QIAzol Lysis Reagent and miRNeasy Mini kits (Qiagen, Valencia (CA), USA) according to the manufacturer's recommendations. RNA concentrations were determined using NanoDrop™ One Microvolume UV-Vis Spectrophotometer (Thermo Fisher Scientific). cDNA for miRNA expression was synthesized from 2 μg of total RNA using the miScript® II RT Kit (Qiagen). The expression levels of *miR-26b* (primer assay ID Hs_miR-26b_1, MS00003234, Qiagen) and *miR-206* (primer assay ID Hs_miR-206_1, MS00003787, Qiagen) were measured by real-time quantitative PCR (qPCR) qPCR using miScript SYBR® Green PCR Kit (Qiagen) for 40 cycles of denaturation (15 s, 94°C), annealing (30 s, 55°C), and extension (30 s, 70°C) with an initial activation step (15 min 94°C) on a QuantStudio 3 Real-Time PCR (Applied Biosytems, Thermo Fisher Scientific). The expression level of RNU49 (primer assay Hs_SNORD49A_11, MS00014028, Qiagen) was used as internal miRNA control. All experiments were performed in triplicate and analyzed using the $2^{-\Delta Ct}$ method. Results represent the mean values of three independent assays.

2.7 | RNA extraction and real-time qPCR

SKOV3 or HUVECs (2×10^5 cells/well) were seeded in 35-mm dishes in a complete culture medium. Selected experiments were carried out in SKOV3 transfected with miR-26b as detailed in the miRNA transfection method. Cells were washed in PBS and total RNA was extracted using the RNeasy Mini Kit (Qiagen, Hilden, Germany). RNA concentrations were determined using a NanoDrop™ One Microvolume UV-Vis spectrophotometer (Thermo Fisher Scientific). cDNA was generated from 1 μg total RNA using the Maxima first-strand cDNA synthesis kit with dsDNase (Thermo Fisher Scientific, Waltham, USA) according to the manufacturer's instructions. The relative quantification of genes of interest was performed by qPCR using SYBR Green PCR Master Mix for 40 cycles of denaturation (15 s, 95°C), annealing (30 s, 60°C), and extension (30 s, 72°C) on a QuantStudio 3 Real-Time PCR (Applied Biosystems, Thermo Fisher Scientific). Primer sequences were the following: *PFKFB3* (forward) GCGTCCCCACAAAAGTGTTC and (reverse) CCGGACTTTCATGGCTTCCT; *GAPDH* (forward) CACCATCTTCCAGGAGCGAG and (reverse) CCTTCTCCATGGTGGTGAAGAC. *GLUT1* (forward) GATTCCCAAGTGTGAGTCGC and (reverse) GACATCATTGCTGGCTGGAG. Target genes were normalized to *GAPDH* and analyzed using the $2^{-\Delta Ct}$ method.

2.8 | Plasmid construction

The 3′-UTR of human *PFKFB3*, containing miR-26b and miR-206 binding sites, was PCR-amplified from genomic DNA and cloned between *XhoI* and *XbaI*, downstream of the firefly luciferase gene in the pmirGLO Dual-Luciferase miRNA Target Expression vector (Promega, Madison, WI, USA). Primer sequences used for cloning were the following: *PFKFB3* UTR fwd 5′-AGCTTACTCGAGGGCAGAC GTGTCGGTTCCATTC-3′ (*XhoI*); *PFKFB3* UTR rev 5′-T ACTAGTCTAGATTTACTTCGTCCATGTATTTCAACC AGG-3′ (*XbaI*).

2.9 | Luciferase reporter assay

SKOV3 (5×10^4 cells/well) were seeded in 24-well plates in a complete culture medium. After 24 h, cells were transfected with 500 ng/well pmirGLO-PFKFB3 3′ UTR in the presence or absence of miRNA-206, miRNA-26b, or miRNA-NC (30 nM, 15 pmol/well) using Lipofectamine3000 (Life Technologies Inc.) for 48 h in a complete culture medium. After transfection, cells were lysed in passive lysis buffer (Promega), and luciferase activities were measured with the Dual-Glo® Luciferase Assay System (Promega) using a luminometer (TD 20/20, Promega), according to the manufacturer's instructions. Firefly luciferase activity was normalized to that of

Renilla luciferase. Four wells of each specific condition were transfected to obtain the mean luciferase activity of each experiment. Results are expressed versus miRNA-NC (miRNA negative control) and represent the mean values of 6 independent experiments.

2.10 | Chemicals

3PO was purchased from Tocris Bioscience (Bristol, UK). Other chemicals were purchased from Sigma.

2.11 | Statistical analysis

All experiments were performed in at least 3 independent replicates; results are presented as mean values, with error bars representing the standard error (SEM) of the average value. Statistical analysis was performed using Graph Pad Prism 6 (Graph Pad Software Inc., La Jolla, CA, USA). Student's *t*-test was used to compare the means of two independent groups. One-way ANOVA followed by Dunnett's, Tukey's, or Bonferroni's *post hoc* tests were used for multiple comparisons. A p-value of $<.05$ was considered statistically significant.

3 | RESULTS

3.1 | The glycolytic protein PFKFB3 is involved in SKOV3 proliferation and migration

PFKFB3 has been found to be overexpressed in several human cancer tissues, including ovarian cancer,[8] but little is known about the functional role of PFKFB3 in ovarian cancer cells.

We first analyzed the effects of the selective PFKFB3 inhibitor 3PO on the proliferation and migration of SKOV3, a highly invasive EOC cell line expressing PFKFB3 at higher levels compared to non-cancer HUVECs (Figure 1A,B). In proliferating cells, treatment with 3PO significantly decreased SKOV3 proliferation in a concentration- and time-dependent manner. At the highest concentration tested (40 μM), 3PO effect was already detectable after 24 h, whereas a lower concentration (20 μM) was effective at later time points (Figure 1C). Moreover, treatment with 40 μM 3PO inhibited FCS-induced SKOV3 migration evaluated by a chemotaxis assay (Figure 1D) in a time frame that did not affect cell morphology (Figure 1E).

These results suggest that the glycolytic regulator PFKFB3 plays a key role in SKOV3 malignancy.

3.2 | MiR-206 and miR-26b overexpression downregulated PFKFB3 protein levels in EOC cell lines

MiRNAs are emerging controllers of glycolytic metabolism in cancer cells, and deregulation of miRNA expression levels has been linked to increased levels of glycolytic proteins including PFKFB3 and GLUT1.[19] In particular, miR-206 and miR-26b have been reported to directly target PFKFB3 in different cancer cell lines.[21,23]

Thus, to explore the regulatory functions of miRNAs in serous EOC cells, we first measured the endogenous expression of *miR-206* and *miR-26b* in SKOV3 cells. We found barely detectable levels of *miR-206* and higher levels of *miR-26b* (Figure 2A). Using a luciferase assay, we showed that miR-26b and even more so miR-206 decreased the 3′ UTR of *PFKFB3* reporter activity, suggesting that both miRNAs negatively regulated *PFKFB3* expression (Figure S1). Accordingly, exogenously added miR-26b and miR-206 mimics decreased PFKFB3 levels in a concentration-dependent manner (0.3–37 nM, Figure 2B). The effect of miR-206 was significantly different with respect to miR-negative control (miR-NC) already at the 3 nM concentration. In addition, treatment with the miR-26b inhibitor (Anti-miR-26b, 0.3–37 nM) concentration-dependently increased PFKFB3 levels compared to negative control (Anti-miR-NC; Figure 2C). However, in line with barely detectable *miR-206* endogenous levels, no changes in PFKFB3 levels were observed in cells transfected with the miR-206 inhibitor (Anti-miR-206) at any concentration tested (0.3–37 nM). Overall, these data suggest different roles for miR-26b and miR-206 in the functional regulation of SKOV3 cells.

Similar findings were collected in two additional OC cell lines. We showed that *miR-26b* was more expressed than *miR-206* in both OVCAR5 and CAOV3 cell lines (Figure 3A). In addition, similarly to what was observed in SKOV3, treatment with exogenous miR-26b and miR-206 mimics (37 nM) negatively regulated the amount of PFKFB3 in these cell lines (Figure 3B,C).

3.3 | miR-26b overexpression enhanced GLUT-1 protein levels in SKOV3

The glucose transporter GLUT1 is the first rate-limiting step in glucose utilization in tissues that rely on glycolysis as a source of energy such as cancer cells.[6] A recent study reported a negative regulatory effect of miR-26b on both GLUT1 and PFKFB3 in osteosarcoma cells.[23] Hence, we hypothesized that shared miRNAs would contribute to the post-transcriptional regulation of proteins of the glycolytic pathway. Unexpectedly, we found that miR-26b overexpression (0.3–37 nM) increased GLUT1

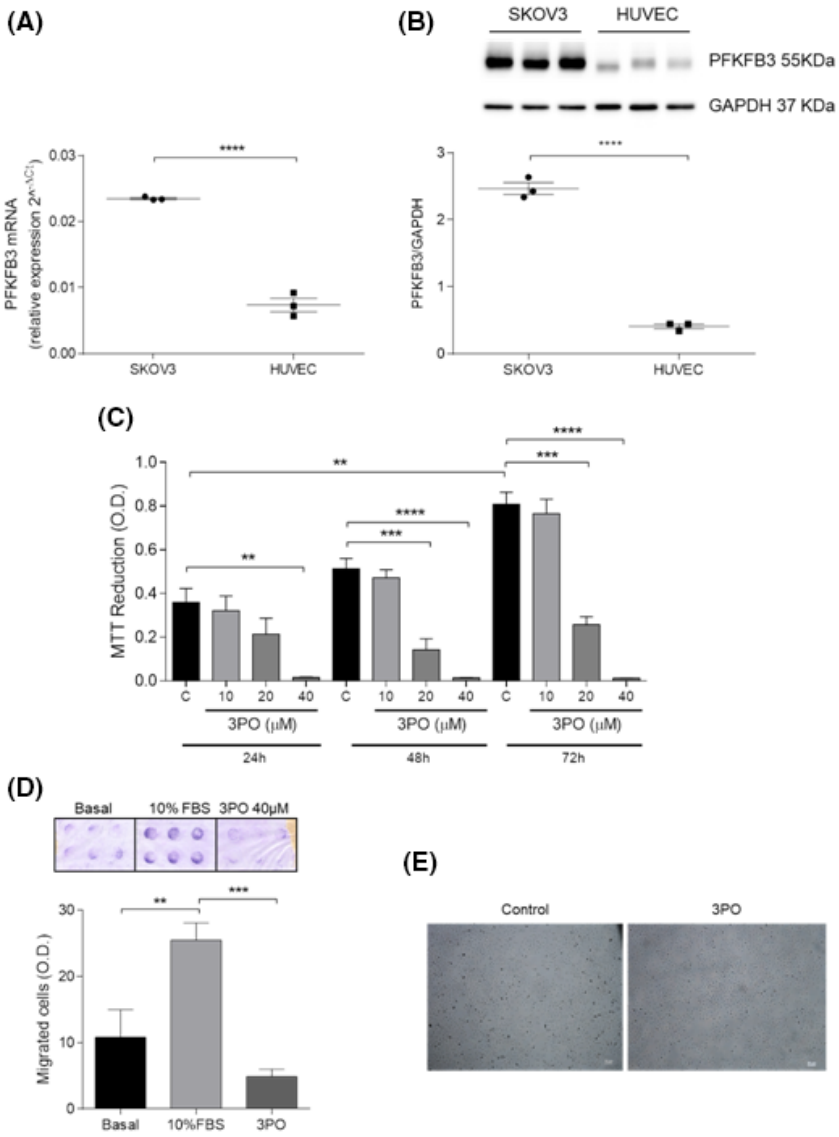

FIGURE 1 The PFKFB3 inhibitor 3PO suppressed SKOV3 proliferation and migration. (A and B) SKOV3 cells and HUVECs (2.0×10^5 cells/well) were seeded in 35-mm dishes and incubated in a complete culture medium. (A) *PFKFB3* mRNA levels were measured by qPCR and normalized to GAPDH. Data are expressed as mean ± SEM of 3 independent samples run in triplicate. ***$p < .001$, *t*-test. (B) *Upper panel*. Representative Western blot showing immunodetection of PFKFB3. *Lower panel*. Densitometric analysis of bands normalized to GAPDH levels. Data are expressed as mean ± SEM of 3 independent samples. ****$p < .001$, *t*-test. (C) SKOV3 cells (2.5×10^3/well) were plated in 96-well plates and incubated in a complete culture medium in the presence or absence of 3PO (10–40 μM) for 24–72 h. Cell proliferation was measured by MTT assay. (C) 10% FCS. Data are expressed as mean ± SEM of 3 independent experiments performed in quadruplicate; **$p < .01$, ***$p < .001$, ****$p < .0001$, one-way ANOVA, Dunnett's post hoc test. (D) *Upper panel*. Representative image of SKOV3 migration in response to 40 μM 3PO in a modified 48-well Boyden chamber after 6 h incubation at 37°C. Basal migration (without chemoattractant stimulus): 0.1% albumin. *Lower panel*. Cell migration is shown as optical density values (O.D., arbitrary units). Each independent experiment was performed in sextuplicate. Data are expressed as mean ± SEM of 3 independent experiments; **$p < .01$, ***$p < .001$, one-way ANOVA, Bonferroni *post hoc* test. (E) SKOV3 cells (2×10^5/well) were seeded in 35-mm dishes and incubated in a complete culture medium in the presence or absence of 3PO (40 μM) for 6 h. Representative images obtained with an inverted bright-field microscope (Nikon Eclipse-Ti) equipped with a digital camera; scale bar: 50 μm

protein levels compared to miR-NC in a concentration-dependent manner (Figure 4A). Conversely, miR-206 did not change GLUT-1 protein expression (Figure 4B), suggesting diverging post-transcriptional regulation of glycolytic proteins levels in SKOV3 cells. To investigate the mechanisms of miR-26b-induced GLUT1 expression, we analyzed the levels of *GLUT1* mRNA upon transfection with miR-26b in SKOV3 cells. As shown in Figure 4C, we found no differences in *GLUT1* mRNA levels in miR-26b-overexpressing cells with respect to control. These data suggest that miR-26b could either directly or indirectly affect GLUT1 at a post-translational level.

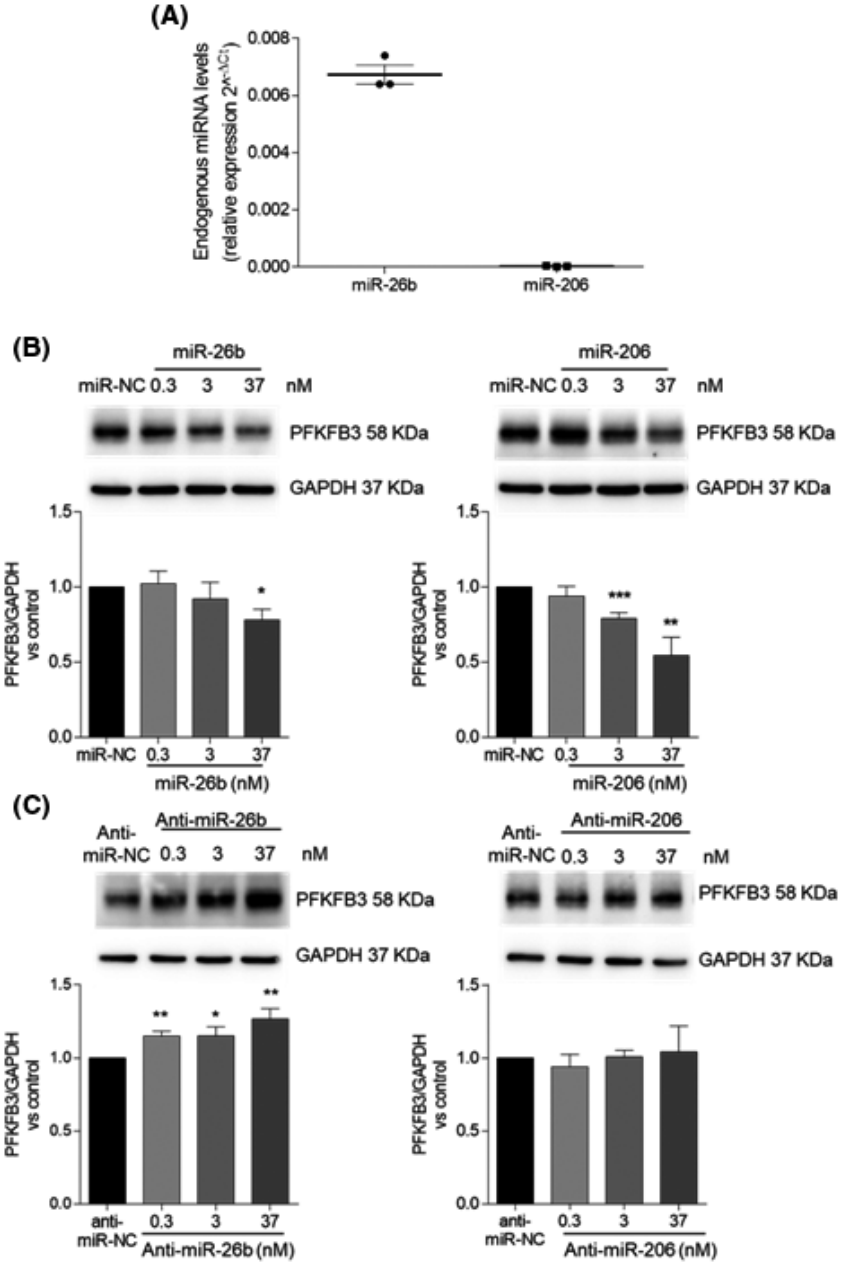

FIGURE 2 miR-26b and miR-206 negatively regulate PFKFB3 protein expression in SKOV3 cells. (A) Endogenous levels of *miR-206* and *miR-26b*. Cells (2.0×10^5/well) were seeded in 35-mm dishes in a complete culture medium. After 48 h, the medium was replaced with a fresh one containing 5% FCS. Expression levels of miRNA were measured by qPCR and normalized to RNU49 internal reference. Data are expressed as mean ± SEM of 3 independent experiments run in triplicate. (B and C) miR-26b and 206 overexpression reduced while miR-26b inhibitor (Anti-miR) increased PFKFB3 protein levels in a concentration-dependent manner. SKOV3 (1.0×10^5 cells/well) were seeded in 12-well plates in a complete culture medium and, after 24 h, transfected with miR-mimics (0.3–37 nM, B) or Anti-miR (0.3–37 nM, C) for 72 h in RPMI with 5% FCS. miR-NC or Anti-miR-NC (37 nM) were used as controls. *Upper panels*: Representative Western blot showing immunodetection of PFKFB3. *Lower panels*: Densitometric analysis of bands, normalized to GAPDH levels, expressed versus control. Data are the mean ± SEM of 3 to 5 independent experiments. (B) $^*p < .05$, $^{**}p < .01$, $^{***}p < .001$ versus miR-negative control (miR-NC); *t*-test. (C) $^*p < .05$, $^{**}p < .01$ versus Anti-miR-NC; *t*-test

3.4 | miRNA-206 transfection reduced SKOV3 proliferation and migration

To further investigate the effects of miR-26b and miR-206 on SKOV3 function, we focused on cell proliferation and invasiveness, two important indices of cell malignancy. The exogenous introduction of miR-206 mimics inhibited SKOV3 proliferation over time by about 35% (Figure 5A), with only a modest apoptosis-inducing effect (*data not shown*). In contrast, miR-26b mimics had no effect on SKOV3 proliferation

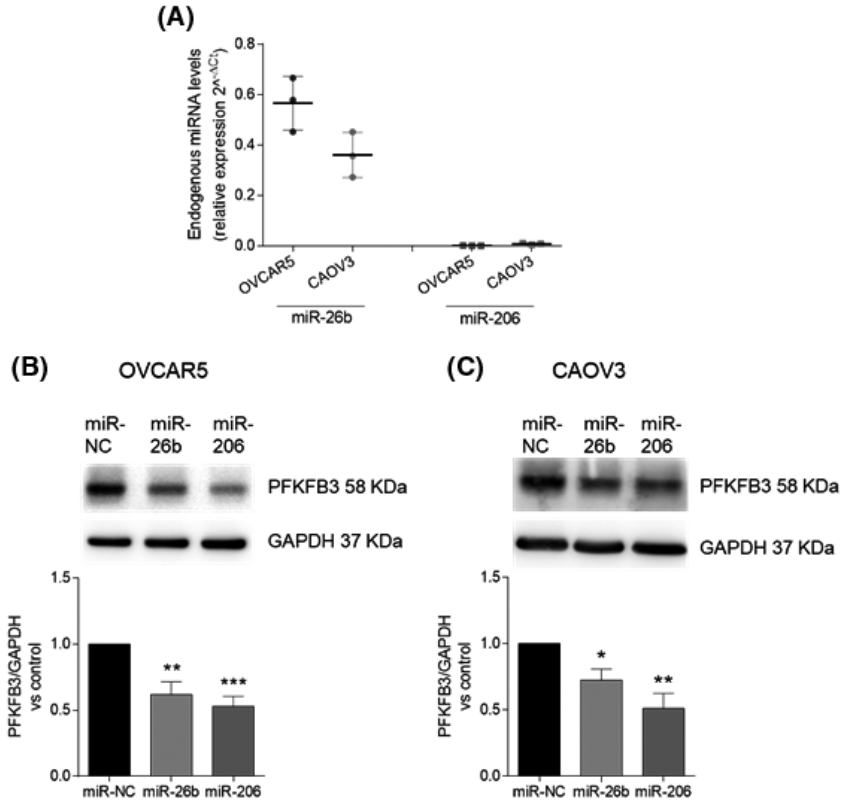

FIGURE 3 miR-26b and miR-206 negatively regulate PFKFB3 protein expression in OVCAR5 and CAOV3 cells. (A) Endogenous levels of *miR-206* and *miR-26b*. OVCAR5 and CAOV3 (2.0×10^5 cells/well) were seeded in 35-mm dishes in a complete culture medium. After 48 h, the medium was replaced with fresh one containing 5% FCS for 24 h. Expression levels of miRNA were measured by qPCR and normalized to RNU49 internal reference. Data are expressed as mean ± SEM of 3 independent experiments. (B and C) miR-26b and miR-206 overexpression reduced PFKFB3 protein levels. OVCAR5 and CAOV3 (1.0×10^5 cells/well) were seeded in 12-well plates in a complete culture medium and, after 24 h, transfected with miR-26b or miR-206 (37 nM) for 72 h in RPMI with 5% FCS. miR-NC was used as control. *Upper panels*. Representative Western blot showing immunodetection of PFKFB3. *Lower panels*. Densitometric analysis of bands, normalized to GAPDH levels, expressed versus control. Data are the mean ± SEM of 4 independent experiments. *$p < .05$, **$p < .01$, ***$p < .001$ versus miR-negative control (miR-NC); *t*-test

(Figure 5A). This can be at least in part explained by the non-overlapping effects of miR-26b and miR-206 on PFKFB3 and GLUT1 expression. SKOV3 migration in response to 10% FCS was significantly decreased in cells overexpressing miR-206 compared to those transfected with non-specific miRNA (miR-NC, 37 nM; Figure 5B). Conversely, miRNA-26b did not decrease cell migration toward 10% FCS but even enhanced SKOV3 invasive properties as evaluated by increased spontaneous migration under basal conditions, i.e., in the absence of chemoattractant stimuli (Figure 5B).

3.5 | miR-206 reduced while miR-26b increased FAK expression in SKOV3

Based on the above results, we hypothesized an opposite effect of miR-206 and miR-26b on key proteins involved in cancer cell migration. In particular, the cytoplasmatic non-receptor protein tyrosine kinase FAK is overexpressed and/or over-phosphorylated in multiple cancer cells and is involved in the regulation of cell proliferation, survival, and migration.[28–30] Moreover, recent findings highlighted that FAK activity can be directly or indirectly regulated by miRNAs.[31]

Therefore, in order to identify a possible mechanism underlying the diverging effects of miR-206 and miR-26b on SKOV3 motility, we measured the expression of total FAK and FAK phosphorylated at Tyr 576/577, which results in full activation of FAK enzyme activity.[32] Western blot analysis showed that overexpression of miR-206 decreased, while that of miR-26b increased total and p-FAK 576/577 protein levels versus miR-negative control (miR-NC), respectively, in a concentration-dependent manner (0.3–37 nM, Figure 6). Thus, in line with the migration outcome, miR-206 and miR-26b induced opposite effects on the levels of FAK and its phosphorylation. To further explore the

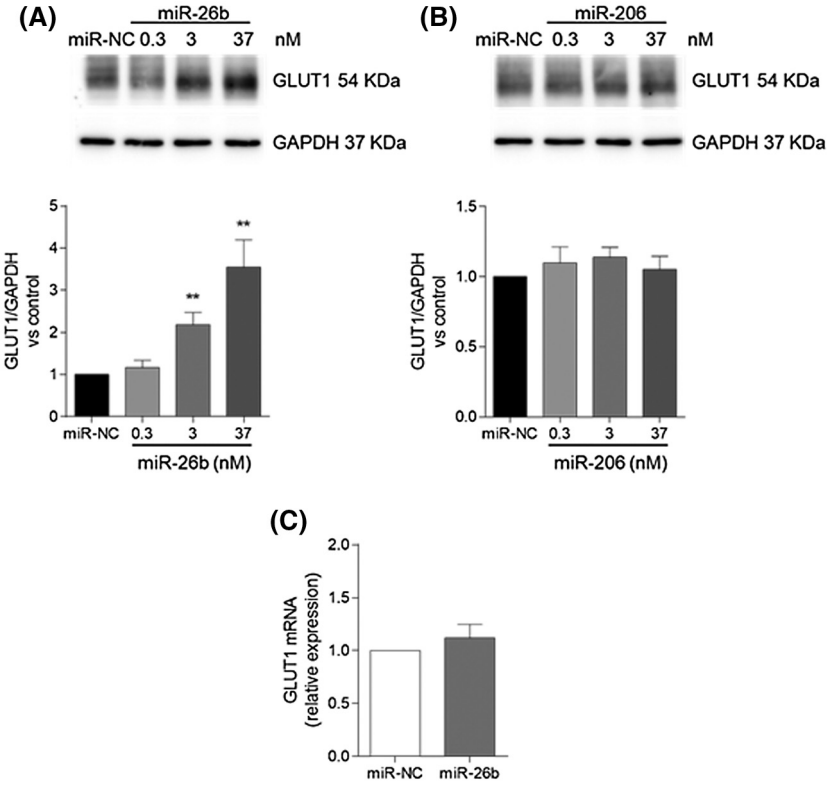

FIGURE 4 miR-26b overexpression increased GLUT1 protein levels in a concentration-dependent manner. (A and B) SKOV3 (1.0×10^5 cells/well) were seeded in 12-well plates in a complete culture medium and, after 24 h, transfected with miR-26b (A) or miR-206 (B, both 0.3–37 nM) in RPMI with 5% FCS for 72 h. miR-NC (37 nM) was used as a control. *Upper panels*: Representative Western blot showing immunodetection of GLUT1. *Lower panel*: Densitometric analysis of bands, normalized to GAPDH levels, expressed versus miR-NC. Data are expressed as mean ± SEM of 3–5 independent experiments. $^{**}p < .01$ versus miR-NC, *t*-test. (C) SKOV3 (2.0×10^5 cells/well) were seeded in 35-mm dishes in a complete culture medium and, after 24 h, transfected with miR-26b (37 nM) in RPMI with 5% FCS for 72 h. miR-NC (37 nM) was used as a control. *GLUT1* mRNA levels were measured by q-PCR and normalized to GAPDH. The expression level of miR-NC was assigned a value of 1. Data are expressed as mean ± SEM of 3 independent experiments run in duplicate

mechanism of miR-26b-mediated SKOV3 migration, we assessed the effect of the PFKFB3 inhibitor 3PO in miR-26b-overexpressing SKOV3 cells. Treatment with 3PO did not significantly prevent the increased migration of miR-26b-transfected SKOV3 cells (Figure 6C). Overall, these data suggest that a PFKFB3-independent pathway is involved in the miR-26b pro-migratory effect.

3.6 | miR-206 and miR-26b induced opposite effects on OVCAR5 and CAOV3 migration

The relevance of the antimigratory potential of miR-206 was confirmed in experiments carried out in OVCAR5 and CAOV3 cells. Similar to what was observed in SKOV3 cells, transfection with miR-206 but not miR-26b mimics (37 nM) decreased total FAK protein levels versus miR-negative control (miR-NC, 37 nM) in OVCAR5 and CAOV3 cells (Figure 7A,B). Accordingly, miR-206 but not mir-26b decreased FCS-induced EOC cell migration with respect to miR-NC (Figure 7C,D). The miR-26b mimic even increased total FAK levels and OVCAR5 spontaneous migration in the absence of chemoattractant stimuli (Figure 7A,C). Overall, these data suggest a unique antimigratory potential of miR-206 through the PFKFB3/FAK axis.

4 | DISCUSSION

Dysregulation of transporters and enzymes involved in glycolytic metabolism, namely GLUT1 and PFKFB3, is a feature of proliferating invasive cancer cells that adapt through multiple mechanisms their metabolic profile to sustain the increased energy requirement.[33,34] MiRNAs directly or indirectly regulate proteins of the glycolytic pathways, thus emerging as novel therapeutic targets to control cancer growth and invasiveness.[19,35,36]

In this study, we showed that restoration of miR-206 expression inhibited proliferation and migration of EOC cell lines including SKOV3, OVCAR5, and CAOV3 by

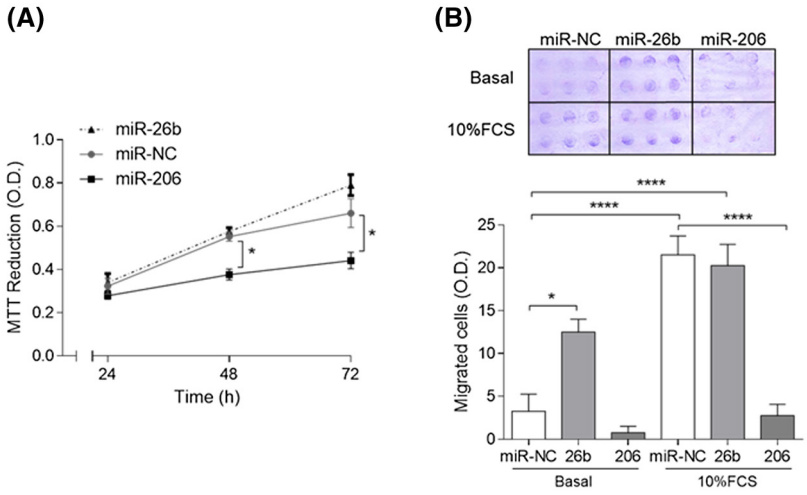

FIGURE 5 miR-206 but not miR-26b transfection reduced SKOV3 cell migration and proliferation. Cells (2×10^5/well) were seeded in 35-mm dishes in a complete culture medium and, after 24 h, transfected with miR-26b or miR-206 (37 nM) in RPMI with 5% FCS for 72 h. miR-NC (37 nM) was used as a control. (A) Transfected SKOV3 were seeded (2.5×10^3 cells/well) in 96-well plates and re-transfected in a complete medium with miRNAs (37 nM) for 24–72 h. Cell proliferation was measured by MTT assay. Data are expressed as mean ± SEM of 3 independent experiments performed in quadruplicate; *$p < .05$, *t*-test. (B) Migration of transfected SKOV3 cells was measured in a chemotaxis assay under basal conditions or using 10% FCS as a chemoattractant agent. *Upper panel*: Representative image of SKOV3 migration in a modified 48-well Boyden chamber after 6-h incubation at 37°C. Basal migration (without chemoattractant stimulus): 0.1% albumin. *Lower panel*: Cell migration is shown as optical density values (O.D., arbitrary units). Data are expressed as mean ± SEM of 4 independent experiments performed in sextuplicate. *$p < .05$, ****$p < .0001$; *t*-test

downregulating PFKFB3 levels. Similar to miR-206, miR-26b also directly targeted *PFKFB3*, but the decreased PFKFB3 protein levels related to miR-26 overexpression had no functional consequences in the EOC cell lines tested. The opposite modulation of FAK expression and activation by miR-206 and miR-26b reported herein may represent a possible mechanism for the diversity of proliferation and migration outcomes in EOC cells following treatment with the two miRNAs.

It is widely recognized that specific miRNAs are aberrantly expressed or downregulated in neoplastic cells or tissues, supporting their role as oncogenes or tumor suppressors, respectively.[37] We, here, report barely detectable levels of *miR-206* and higher levels of *miR-26b* in EOC cells. Decreased levels of miR-206 compared to controls were already found in cancer tissues as well as in several ovarian cancer cell lines including SKOV3, which showed the lowest miR-206 levels.[38] Interestingly, E2 concentration-dependently decreases miR-206 and miR-26b levels in breast cancer cells.[20,21] In addition, miR-206 is downregulated in ERα-positive tissues as well as in MCF7 cells with respect to ERα-negative cells, and ERα agonists may modulate this effect.[24,25] This is in line with the direct effect of this tumor-suppressor miRNA on the negative regulation of estrogen-responsive genes, including ERα.[25,39]

However, the evidence on the functional role of miR-206 and miR-26b in ovarian cancer is limited[38,40,41]; in particular, their effects on glycolytic proteins and the potential functional consequences have not been investigated in detail. We first focused on the glycolysis regulator PFKFB3, which is overexpressed in SKOV3 cells, upregulated by E2 via post-transcriptional mechanisms (*data not shown*), and involved in cell growth and migration. miR-26b and even more so miR-206 decreased the luciferase activity of EOC transfected cells, supporting their direct interaction with the 3′-UTR of *PFKFB3* transcript/mRNA, as already observed in other cancer cells.[21,23] Accordingly, transfection of SKOV3 cells with miR-26b and miR-206 significantly reduced PFKFB3 protein expression compared to miR-negative control (Figure 2B). The effect of miR-206 was detectable at lower miR-mimic concentrations, suggesting a higher affinity for the target.[42] Moreover, in line with the different endogenous levels of target miRNAs, only anti-miR-26b increased PFKFB3 protein levels, counteracting the effect of endogenous *miR-26b* (Figure 2C).

Since miRNAs have the potential to simultaneously regulate the expression of multiple proteins,[43] and several miRNAs directly or indirectly suppress GLUT1-mediated glucose uptake with functional consequences on cell proliferation,[19,44] we explored whether miR-26b and miR-206 could have a wider effect on glycolytic proteins by modulating the expression of the glucose transporter GLUT1. At variance with miR-206, which did not affect GLUT1, exogenously added miR-26b-upregulated

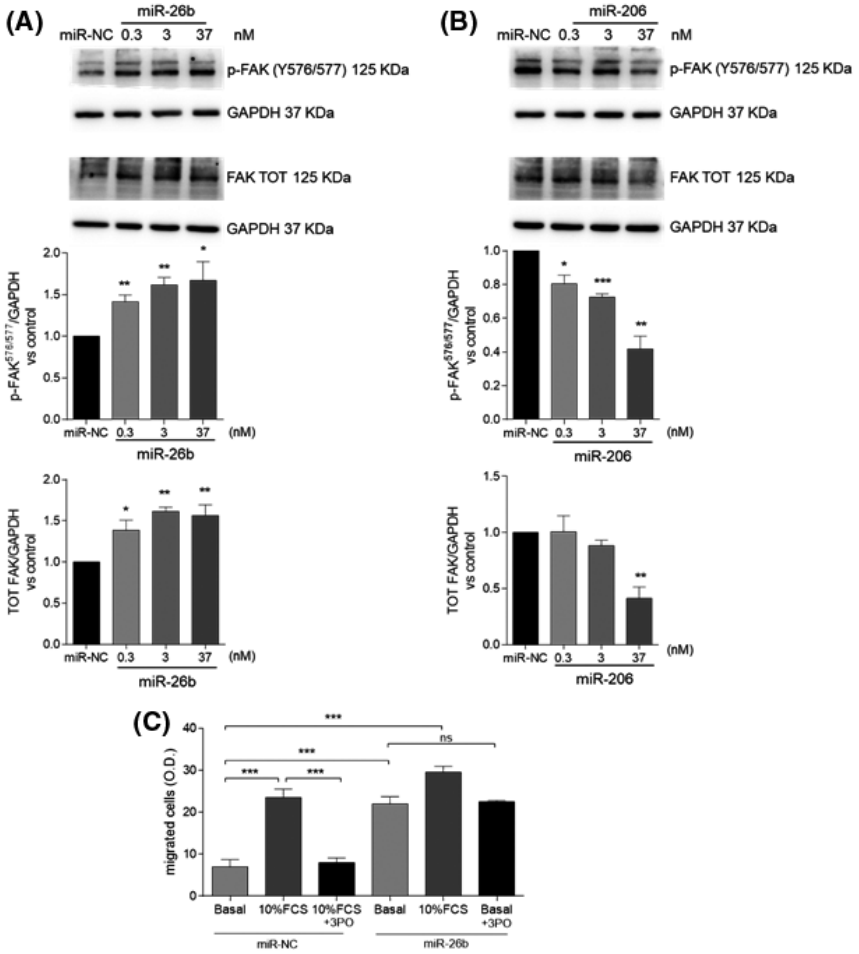

FIGURE 6 Opposite effects of miR-26b and miR-206 on p-FAK$^{Y576/577}$ and total FAK protein levels. (A and B) SKOV3 (1.0×10^5 cells/well) were seeded in 12-well plates in a complete culture medium and, after 24 h, transfected with miR-26b (A) or miR-206 (B; both 0.3–37 nM) in RPMI with 5% FCS for 72 h. MiR-NC (37 nM) was used as a negative control. *Upper panels*: Representative Western blot showing immunodetection of p-FAK$^{Y576/577}$ and total FAK. *Lower panel*: Densitometric analysis of bands, normalized to GAPDH levels, expressed versus miR-NC. Data are expressed as mean ± SEM of 3 independent experiments. *$p < .05$, **$p < .01$, ***$p < .001$ versus miRNA-NC; one-way analysis of variance (ANOVA), Dunnett's *post hoc* test. (C) The PFKFB3 inhibitor 3PO did not suppress miR-26b-induced SKOV3 migration. Cells (2.0×10^5/well) were seeded in 35-mm dishes in a complete culture medium and, after 24 h, transfected with miR-26b (37 nM) in RPMI with 5% FCS for 72 h. miR-NC (37 nM) was used as a control. Migration of transfected SKOV3 cells in response to 40 μM 3PO was measured in a chemotaxis assay under basal conditions or using 10% FCS as a chemoattractant agent. Basal migration (without chemoattractant stimulus): 0.1% albumin. Cell migration is shown as optical density values (O.D., arbitrary units). Data are expressed as mean ± SEM of three independent experiments performed in sextuplicate: ***$p < .001$, one-way analysis of variance (ANOVA), Tukey's *post hoc* test; *ns*: nonsignificant

GLUT1 protein but not mRNA levels, suggesting that miR-26b could affect GLUT1 at a post-translational level.[45] More important, miR-206 but not miR-26b suppressed SKOV3 cell growth over time and significantly decreased motility, suggesting that the binding specificity to multiple targets dictates the overall tumor suppressor effects of each miRNA.

Previous studies showed opposite functional effects of miR-26b on cell proliferation and migration according to cell type.[23,46] For instance, miR-26b inhibits osteosarcoma cell growth and migration,[23] while it increases the migration of mesenchymal stem cells by enhancing p-Akt and p-FAK protein levels *via* downregulation of phosphatase and tensin homolog (PTEN).[46] Notably, several studies suggest that specific miRNAs, rather than directly suppressing FAK expression by binding to FAK mRNA, indirectly regulate FAK expression and activity.[31] In addition, Zhao et al. recently reported that GLUT1 promotes the malignant behavior of non-small cell lung cancer through integrin β1/Src/FAK phosphorylation at Tyr 576/577,[13] further suggesting a link between glucose metabolism and cell motility.

Hence, we focused on FAK, which is overexpressed in ovarian as well as other cancers and plays a pivotal role

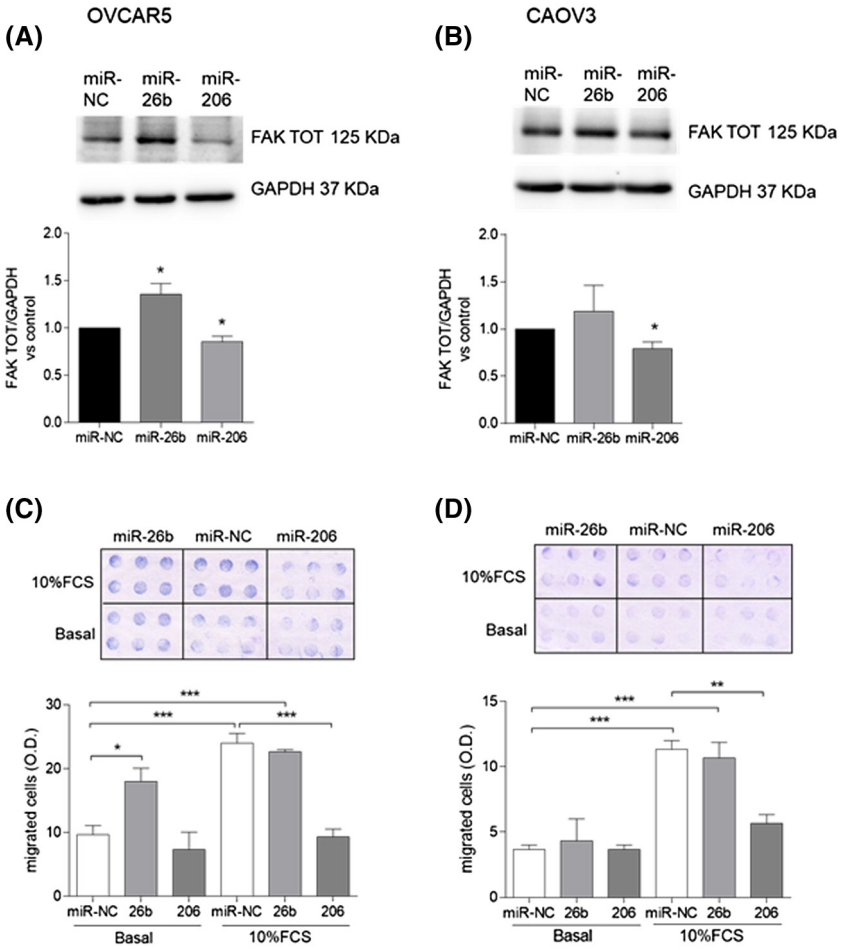

FIGURE 7 Opposite effects of miR-26b or miR-206 on total FAK protein levels in OVCAR5 and CAOV3 cells. Cells (2.0×10^5 cells/well) were seeded in 35-well plates in a complete culture medium and, after 24 h, transfected with miR-26b or miR-206 (37 nM) for 72 h in RPMI with 5% FCS. miR-NC was used as a control. (A and B) *Upper panels*: Representative Western blot showing immunodetection of total FAK. *Lower panels*: Densitometric analysis of bands, normalized to GAPDH levels, expressed versus control. Data are the mean ± SEM of 3–4 independent experiments. *$p < .05$ versus miR-negative control (miR-NC); *t*-test. (C and D) Migration of transfected OVCAR5 and CAOV3 cells was measured in a chemotaxis assay under basal conditions or using 10% FCS as a chemoattractant agent. *Upper panels*: Representative image of cell migration in a modified 48-well Boyden chamber after 6-h incubation at 37°C. Basal migration (without chemoattractant stimulus): 0.1% albumin. *Lower panels*: Cell migration is shown as optical density values (O.D., arbitrary units). Data are expressed as mean ± SEM of 3 independent experiments performed in sextuplicate. *$p < .05$, **$p < .01$, ***$p < .001$; one-way analysis of variance (ANOVA), Tukey's *post hoc* test

in the regulation of cell adhesion, motility, proliferation, survival, as well as resistance to chemotherapy.[28–30,47] Interestingly, we found that miR-26b overexpression increased, while miR-206 decreased total and Y576/577 FAK levels in SKOV3. The unique effect of miR-206 compared to that of miR-26b on FAK was confirmed in other EOC cell lines (Figure 7). These findings may account, at least in part, for the specific inhibitory effect of miR-206 on EOC cell migration reported herein and are in line with previous evidence in rhabdomyosarcoma cells, where miR-206 inhibits cell invasiveness by targeting MET proto-oncogene, receptor tyrosine kinase (c-MET) and indirectly reducing FAK phosphorylation.[48] Accordingly, a recent study showed that miR-206 directly targets and inhibits the *ITGA2* gene encoding the integrin receptor CD49b, an upstream regulator of FAK that promotes breast cancer metastasis.[49] Overall, it is conceivable that miR-206 behaved as an oncosuppressor endowed with antimigratory properties in EOC cells by acting as a potent inhibitor of PFKFB3 and downstream FAK. By contrast, in the same setting, transfection of miR-26b resulted in a glycolytic phenotype that fostered FAK activation and enhanced spontaneous migration by increasing GLUT1, despite a weak negative regulation of PFKFB3 protein levels. In line with the previous findings showing that FAK expression can be modulated at a post-translational level,[50,51] we hypothesize that miR-26b indirectly enhanced FAK as well as GLUT1 levels. However, we cannot exclude that miR-26b directly increased GLUT1 and FAK expression by upregulating

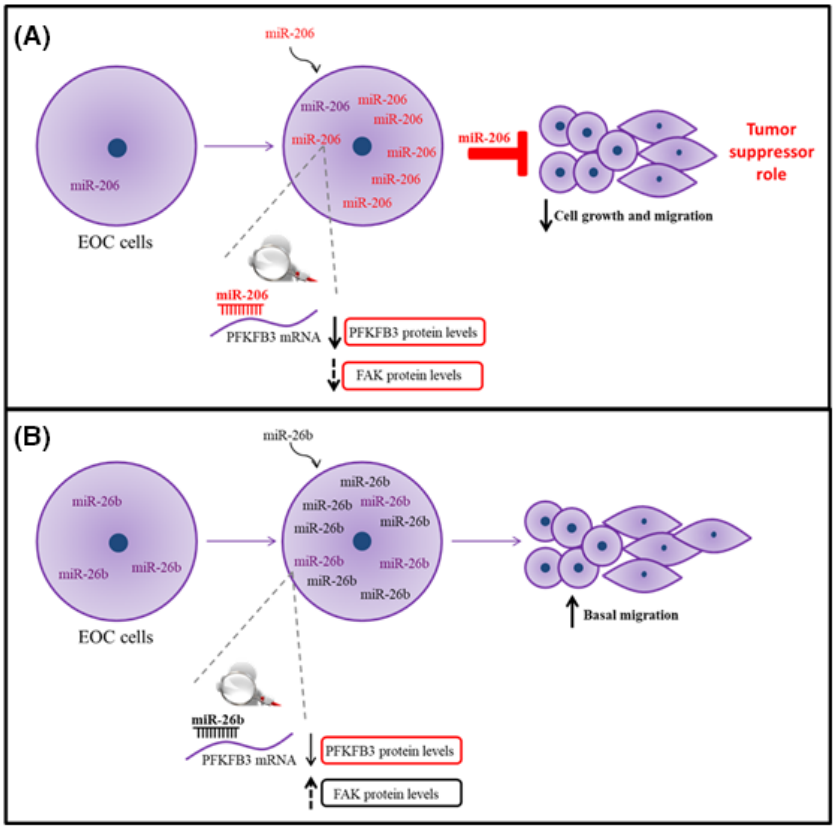

FIGURE 8 Tumor suppressor role of miR-206 in EOC cells. In cells expressing low levels of *miR-206* (A) and high levels of *miR-26b* (B), exogenous administration of miR-206, but not miR-26b, displays anti-migratory and anti-proliferative effects through downregulation of the PFKFB3/FAK axis

protein translation.[52] Remarkably, the PFKFB3 inhibitor 3PO did not counteract the increased basal migration observed in miR-26b-overexpressing cells. These data point to a pivotal functional role of FAK activation in this setting and suggest that inhibition of PFKFB3 alone could not be sufficient to overcome tumor invasiveness in FAK-overexpressing tumors. This working hypothesis is depicted in Figure 8.

It is worth mentioning that the functional role of miR-206 and miR-26b in the setting of tumors appears to be inversely related to their endogenous expression levels, as previously highlighted by others.[41,53] Indeed, several reports showed that ovarian cancer features DNA hypermethylation and miRNA levels could be increased by demethylating agents.[26,54] Understanding the mechanisms involved in the regulation of miR-206 levels and the role of estrogenic agents in this process[55] warrants further research. We are currently assessing the DNA methylation/acetylation patterns of miR-206 and miR-26b in SKOV3 and other EOC cell lines with respect to healthy epithelial cells.

In summary, we provide evidence that miR-206 mimics inhibited the proliferation and motility of several EOC cells acting as negative post-transcriptional regulators of PFKFB3 and downstream FAK. These results support the inverse relation between endogenous miRNA levels and their tumor-suppressive effects and suggest that restoring miR-206 represents a potentially valuable dual anti-PFKFB3/FAK strategy to control the progression of ovarian cancers characterized by FAK overexpression and resistance to chemotherapy.

ACKNOWLEDGMENTS

This work was supported by the University of Padova (PRID Grant 2018 to ChBo) and the Muscular Dystrophy Association (grant 577888 to DS). Open Access Funding provided by Universita degli Studi di Padova within the CRUI-CARE Agreement. [Correction added on May 31, 2022, after first online publication: CRUI-CARE Funding statement has been added.]

DISCLOSURES

No conflict of interest.

AUTHOR CONTRIBUTIONS

Carlotta Boscaro designed and performed the experiments; Marcello Carotti and Dorianna Sandonà created the vector and designed luciferase experiments; Chiara Baggio performed some of the experiments; Lucia Trevisi analyzed and interpreted the data; Andrea Cignarella analyzed and interpreted the data and wrote the manuscript; Chiara Bolego designed the research, analyzed and interpreted the data, and wrote the manuscript and all the authors have read this manuscript.

REFERENCES

1. Moreno-Sánchez R, Rodríguez-Enríquez S, Marín-Hernández A, Saavedra E. Energy metabolism in tumor cells. *FEBS J*. 2007;274:1393-1418.
2. Shi L, Pan H, Liu Z, Xie J, Han W. Roles of PFKFB3 in cancer. *Signal Transduct Target Ther*. 2017;2:e17044.
3. Nowak N, Kulma A, Gutowicz J. Up-regulation of key glycolysis proteins in cancer development. *Open Life Sci*. 2018;13:569-581.
4. Xintaropoulou C, Ward C, Wise A, et al. Expression of glycolytic enzymes in ovarian cancers and evaluation of the glycolytic pathway as a strategy for ovarian cancer treatment. *BMC Cancer*. 2018;18:636.
5. Cho H, Lee YS, Kim J, Chung JY, Kim JH. Overexpression of glucose transporter-1 (GLUT-1) predicts poor prognosis in epithelial ovarian cancer. *Cancer Invest*. 2013;31:607-615.
6. Cantuaria G, Fagotti A, Ferrandina G, et al. GLUT-1 expression in ovarian carcinoma: association with survival and response to chemotherapy. *Cancer*. 2001;92:1144-1150.
7. Kotowski K, Rosik J, Machaj F, et al. Role of PFKFB3 and PFKFB4 in cancer: genetic basis, impact on disease development/progression, and potential as therapeutic targets. *Cancers*. 2021;13:909.
8. Atsumi T, Chesney J, Metz C, et al. High expression of inducible 6-phosphofructo-2-kinase/fructose-2,6-bisphosphatase (iPFK-2; PFKFB3) in human cancers. *Cancer Res*. 2002;62:5881-5887.
9. Mondal S, Roy D, Sarkar Bhattacharya S, et al. Therapeutic targeting of PFKFB3 with a novel glycolytic inhibitor PFK158 promotes lipophagy and chemosensitivity in gynecologic cancers. *Int J Cancer*. 2019;144:178-189.
10. Taylor C, Mannion D, Miranda F, et al. Loss of PFKFB4 induces cell death in mitotically arrested ovarian cancer cells. *Oncotarget*. 2017;8:17960-17980.
11. Boscaro C, Trenti A, Baggio C, et al. Sex differences in the pro-angiogenic response of human endothelial cells: focus on PFKFB3 and FAK activation. *Front Pharmacol*. 2020;11:587221.
12. Zhu W, Ye L, Zhang J, et al. PFK15, a small molecule inhibitor of PFKFB3, induces cell cycle arrest, apoptosis and inhibits invasion in gastric cancer. *PLoS One*. 2016;11:e0163768.
13. Zhao H, Sun J, Shao J, et al. Glucose transporter 1 promotes the malignant phenotype of non-small cell lung cancer through integrin β1/Src/FAK signaling. *J Cancer*. 2019;10:4989-4997.
14. Eelen G, de Zeeuw P, Simons M, Carmeliet P. Endothelial cell metabolism in normal and diseased vasculature. *Circ Res*. 2015;116:1231-1244.
15. Qi C, Pekala PH. The influence of mRNA stability on glucose transporter (GLUT1) gene expression. *Biochem Biophys Res Commun*. 1999;263:265-269.
16. Trenti A, Tedesco S, Boscaro C, et al. The glycolytic enzyme PFKFB3 is involved in estrogen-mediated angiogenesis via GPER1. *J Pharmacol Exp Ther*. 2017;361:398-407.
17. Boscaro C, Carotti M, Albiero M, et al. Non-genomic mechanisms in the estrogen regulation of glycolytic protein levels in endothelial cells. *FASEB J*. 2020;34:12768-12784.
18. Rupaimoole R, Slack FJ. MicroRNA therapeutics: towards a new era for the management of cancer and other diseases. *Nat Rev Drug Discov*. 2017;16:203-222.
19. Subramaniam S, Jeet V, Clements JA, Gunter JH, Batra J. Emergence of microRNAs as key players in cancer cell metabolism. *Clin Chem*. 2019;65:1090-1101.
20. Tan S, Ding K, Li R, et al. Identification of miR-26 as a key mediator of estrogen stimulated cell proliferation by targeting CHD1, GREB1 and KPNA2. *Breast Cancer Res*. 2014;16:R40.
21. Ge X, Lyu P, Cao Z, et al. Overexpression of miR-206 suppresses glycolysis, proliferation and migration in breast cancer cells via PFKFB3 targeting. *Biochem Biophys Res Commun*. 2015;463:1115-1121.
22. He Y, Deng F, Zhao S, et al. Analysis of miRNA-mRNA network reveals miR-140-5p as a suppressor of breast cancer glycolysis via targeting GLUT1. *Epigenomics*. 2019;11:1021-1036.
23. Du JY, Wang LF, Wang Q, Yu LD. miR-26b inhibits proliferation, migration, invasion and apoptosis induction via the downregulation of 6-phosphofructo-2-kinase/fructose-2,6-bisphosphatase-3 driven glycolysis in osteosarcoma cells. *Oncol Rep*. 2015;33:1890-1898.
24. Adams BD, Furneaux H, White BA. The micro-ribonucleic acid (miRNA) miR-206 targets the human estrogen receptor-α (ERα) and represses ERα messenger RNA and protein expression in breast cancer cell lines. *Mol Endocrinol*. 2007;21:1132-1147.
25. Kondo N, Toyama T, Sugiura H, Fujii Y, Yamashita H. miR-206 expression is down-regulated in estrogen receptor α-positive human breast cancer. *Cancer Res*. 2008;68:5004-5008.
26. Iorio MV, Visone R, Di Leva G, et al. MicroRNA signatures in human ovarian cancer. *Cancer Res*. 2007;67:8699-8707.
27. Bolego C, Buccellati C, Radaelli T, et al. eNOS, COX-2, and prostacyclin production are impaired in endothelial cells from diabetics. *Biochem Biophys Res Commun*. 2006;339:188-190.
28. Sood AK, Coffin JE, Schneider GB, et al. Biological significance of focal adhesion kinase in ovarian cancer: role in migration and invasion. *Am J Pathol*. 2004;165:1087-1095.
29. Murphy JM, Rodriguez YAR, Jeong K, Ahn EE, Lim SS. Targeting focal adhesion kinase in cancer cells and the tumor microenvironment. *Exp Mol Med*. 2020;52:877-886.
30. Levy A, Alhazzani K, Dondapati P, et al. Focal adhesion kinase in ovarian cancer: a potential therapeutic target for platinum and taxane-resistant tumors. *Curr Cancer Drug Targets*. 2019;19:179-188.
31. Naser R, Aldehaiman A, Díaz-Galicia E, Arold ST. Endogenous control mechanisms of FAK and PYK2 and their relevance to cancer development. *Cancers*. 2018;10:196.
32. Westhoff MA, Serrels B, Fincham VJ, Frame MC, Carragher NO. SRC-mediated phosphorylation of focal adhesion kinase couples actin and adhesion dynamics to survival signaling. *Mol Cell Biol*. 2004;24:8113-8133.
33. Porporato PE, Dhup S, Dadhich RK, Copetti T, Sonveaux P. Anticancer targets in the glycolytic metabolism of tumors: a comprehensive review. *Front Pharmacol*. 2011;2:49.
34. Tyagi K, Mandal S, Roy A. Recent advancements in therapeutic targeting of the Warburg effect in refractory ovarian cancer: a promise towards disease remission. *Biochim Biophys Acta Rev Cancer*. 2021;1876:188563.

35. Singh PK, Mehla K, Hollingsworth MA, Johnson KR. Regulation of aerobic glycolysis by microRNAs in cancer. *Mol Cell Pharmacol*. 2011;3:125-134.
36. Baranwal S, Alahari SK. miRNA control of tumor cell invasion and metastasis. *Int J Cancer*. 2010;126:1283-1290.
37. Ghafouri-Fard S, Shoorei H, Taheri M. miRNA profile in ovarian cancer. *Exp Mol Pathol*. 2020;113:104381.
38. Dai C, Xie Y, Zhuang X, Yuan Z. MiR-206 inhibits epithelial ovarian cancer cells growth and invasion via blocking c-Met/AKT/mTOR signaling pathway. *Biomed Pharmacother*. 2018;104:763-770.
39. Chen X, Yan Q, Li S, et al. Expression of the tumor suppressor miR-206 is associated with cellular proliferative inhibition and impairs invasion in ERα-positive endometrioid adenocarcinoma. *Cancer Lett*. 2012;314:41-53.
40. Sheng N, Xu YZ, Xi QH, et al. Overexpression of KIF2A is suppressed by miR-206 and associated with poor prognosis in ovarian cancer. *Cell Physiol Biochem*. 2018;50:810-822.
41. Lin J, Zhang L, Huang H, et al. MiR-26b/KPNA2 axis inhibits epithelial ovarian carcinoma proliferation and metastasis through downregulating OCT4. *Oncotarget*. 2015;6:23793-23806.
42. O'Brien J, Hayder H, Zayed Y, Peng C. Overview of microRNA biogenesis, mechanisms of actions, and circulation. *Front Endocrinol*. 2018;9:402.
43. Friedman RC, Farh KK, Burge CB, Bartel DP. Most mammalian mRNAs are conserved targets of microRNAs. *Genome Res*. 2009;19:92-105.
44. Fan JY, Yang Y, Xie JY, Lu YL, Shi K, Huang YQ. MicroRNA-144 mediates metabolic shift in ovarian cancer cells by directly targeting Glut1. *Tumour Biol*. 2016;37:6855-6860.
45. Giorgino F, de Robertis O, Laviola L, et al. The sentrin-conjugating enzyme mUbc9 interacts with GLUT4 and GLUT1 glucose transporters and regulates transporter levels in skeletal muscle cells. *Proc Natl Acad Sci U S A*. 2000;97:1125-1130.
46. Zhu A, Kang N, He L, Li X, Xu X, Zhang H. MiR-221 and miR-26b regulate chemotactic migration of MSCs toward HGF through activation of Akt and FAK. *J Cell Biochem*. 2016;117:1370-1383.
47. Diaz Osterman CJ, Ozmadenci D, Kleinschmidt EG, et al. FAK activity sustains intrinsic and acquired ovarian cancer resistance to platinum chemotherapy. *eLife*. 2019;8:e47327.
48. Yan D, Dong Xda E, Chen X, et al. MicroRNA-1/206 targets c-Met and inhibits rhabdomyosarcoma development. *J Biol Chem*. 2009;284:29596-29604.
49. Adorno-Cruz V, Hoffmann AD, Liu X, et al. ITGA2 promotes expression of ACLY and CCND1 in enhancing breast cancer stemness and metastasis. *Genes Dis*. 2020;8:493-508.
50. Fan Y, Qu X, Ma Y, Liu Y, Hu X. Cbl-b promotes cell detachment via ubiquitination of focal adhesion kinase. *Oncol Lett*. 2016;12:1113-1118.
51. Nguyen N, Yi JS, Park H, Lee JS, Ko YG. Mitsugumin 53 (MG53) ligase ubiquitinates focal adhesion kinase during skeletal myogenesis. *J Biol Chem*. 2014;289:3209-3216.
52. Vasudevan S, Tong Y, Steitz JA. Switching from repression to activation: microRNAs can up-regulate translation. *Science*. 2007;318:1931-1934.
53. Gajek A, Gralewska P, Marczak A, Rogalska A. Current implications of microRNAs in genome stability and stress responses of ovarian cancer. *Cancers (Basel)*. 2021;13:2690.
54. Gu Y, Yang P, Shao Q, et al. Investigation of the expression patterns and correlation of DNA methyltransferases and class I histone deacetylases in ovarian cancer tissues. *Oncol Lett*. 2013;5:452-458.
55. Wu Q, Odwin-Dacosta S, Cao S, Yager JD, Tang WY. Estrogen down regulates COMT transcription via promoter DNA methylation in human breast cancer cells. *Toxicol Appl Pharmacol*. 2019;367:12-22.

SUPPORTING INFORMATION

Additional supporting information may be found in the online version of the article at the publisher's website.

How to cite this article: Boscaro C, Baggio C, Carotti M, et al. Targeting of PFKFB3 with miR-206 but not mir-26b inhibits ovarian cancer cell proliferation and migration involving FAK downregulation. *FASEB J*. 2022;36:e22140. doi:10.1096/fj.202101222R